Submitted to ADVANCED MATERIALS

DOI: 10.1002/adma.((please add manuscript number))
Article type: Communication

Submicron surface-patterned fibers and textiles

By *Tural Khudiyev*[+], *Chong Hou*[+], *Alexander M. Stolyarov* and *Yoel Fink**

Prof. Y. Fink (corresponding author)
Department of Materials Science and Engineering, Massachusetts Institute of Technology, Cambridge, Massachusetts 02139, USA
Institute of Soldier Nanotechnology, Massachusetts Institute of Technology, Cambridge, Massachusetts 02139, USA
Department of Electrical Engineering and Computer Science, Massachusetts Institute of Technology, Cambridge, Massachusetts 02139, USA
E-mail: yoel@mit.edu
Dr. T. Khudiyev, Dr. C. Hou, Prof. Y. Fink
Research Laboratory of Electronics, Massachusetts Institute of Technology, Cambridge, Massachusetts 02139, USA
Dr. A. M. Stolyarov
MIT Lincoln Laboratory, Lexington, MA 02420

+ These authors contributed equally

Keywords: grating, fiber, polymer, patterning, textile

The Lincoln Laboratory portion of this material is based upon work supported by the Assistant Secretary of Defense for Research and Engineering under Air Force Contract No. FA8721-05-C-0002 and/or FA8702-15-D-0001. Any opinions, findings, conclusions or recommendations expressed in this material are those of the author(s) and do not necessarily reflect the views of the Assistant Secretary of Defense for Research and Engineering.

Presently, the worldwide annual production volume of textile fibers is nearly one hundred million metric tons. [1] Most of these fibers undergo chemical treatments to achieve properties such as color, hydrophobicity, antimicrobial, UV-protection and others.[2,3,4,5] These chemical-based textile treatments come with significant societal penalties, including adverse health and environmental effects as well as tremendous energy expenditures.[6,7,8,9,10,11,12,13,14,15,16] Therefore, alternative and sustainable strategies to achieve textile surface functionality is highly desired. Here we present a chemical-free, all-structural fiber surface patterning technique that facilitates textile surface functionality while at the same time being safe, environmentally friendly, and cost effective.

To date, surface patterning of materials at the micro and nanoscales has provided many functions, including diffraction gratings,[17] surface wetting,[18] plasmonic metasurfaces,[19] surface enhanced Raman scattering (SERS),[20] triboelectricity,[21] bio-surface interactions,[22] and others. Various techniques,[23,24] including molding and embossing, masked deposition, optical lithography, e-beam lithography, and scanning probe techniques, have been developed for patterning different features, at length scales ranging from nanometer to millimeter. Present methods have two main shortcomings that preclude their use for textiles. First, to achieve surface-patterned functionalized textiles, fibers need to be produced at km-length scales, at high-throughput, and with uniform cross-sectional features at the micron or submicron scale. Conventional surface patterning techniques, however, cannot simultaneously meet all these requirements. Second, textile materials are primarily polymer-based, while most surface-patterning techniques have been developed for silicon. Alternative substrates, especially flexible polymers, remain challenging to pattern [25,26] due to the highly specific surface chemistry of different polymer classes, their characteristically low elastic moduli, and the difficulties of handling flexible substrates. Here we report on a two-step surface patterning technique called fiber surface patterning (FSP) based on a combination of macro-machining and thermal fiber drawing that 1) enables high spatial resolution (submicron scale) patterning over km-long lengths on flexible substrates with high spatial uniformity (~1%) at speeds that are at least an order of magnitude faster than conventional optical lithography and 2)

completely circumvents the aforementioned problems of patterning soft polymers. Instead of relying on chemical properties, this technique harnesses bulk physical material properties (mechanical, optical, and thermal), thereby eliminating both the need for chemically treating the surfaces and for processing flexible substrates. We demonstrate the broad utility of this method by patterning amorphous and semi-crystalline polymers with widely disparate chemical properties, including fluoropolymers, acrylates, carbonates, and olefins. This fiber surface patterning technique enables a unique set of textile functionalities. As examples, we demonstrate micro-structured fibers and fabrics with directional wetting and structural coloration properties.

Figure 1 illustrates the two-step process of the FSP technique. First, macroscale physical material forming techniques are used to generate sub-mm class features over a cm^2 class surface area on a bulk, rigid substrate called a preform (**Figure 1a-c**). Second, the preform is thermally drawn into a flexible fiber device in a process that reduces the preform cross-sectional features down to submicron while generating a surface area to the m^2 range (Figure 1d-e). In the first step, we investigate three specific types of physical forming techniques: milling, laser cutting, and molding (Figure S1). Each method has its unique attributes and is selected based on the properties of the material to be formed. Milling leverages mechanical properties of materials and works well for stiff materials. It can be utilized to define sub-millimeter features with desired depth/width and can be applied on many common amorphous thermoplastics (*e.g.* polycarbonate (PC), polytetrafluoroethylene (PTFE), poly(methyl methacrylate) (PMMA), etc.) and metals. The laser cutting method leverages optical properties of materials. Most nonmetallic materials are highly absorptive at the CO_2 laser wavelength (10.6 μm), and the cutting process involves three mechanisms: vaporization, melt shearing or chemical degradation-based removal of plastic material. [27] Feature sizes obtained using this technique are several hundred microns. One of the main advantages of laser cutting is its short processing time. It only takes a few seconds to minutes to create features over the entire preform area. Molding is based on thermal material properties. It relies on shaping surface features of materials by melting or softening them under elevated temperature and pressure. This technique is particularly well-suited for surface patterning semi-crystalline

polymers, such as polyvinylidene fluoride (PVDF). Conventional molding methods for plastics limit the feature sizes to hundreds of microns. In the second step, a thermal fiber drawing process is used to scale down the surface pattern of the preform into a flexible surface-patterned fiber (Figure 1d). The preform-to-fiber draw down ratio (DDR) can range from a factor of ten to several hundred. Critically, the surface-patterned feature size is also reduced by the DDR. The principal challenge in this step is reducing the cross-sectional feature size while mitigating surface energy driven deformation of non-equilibrium surface features, such as rectangular trenches. This is achieved by judiciously controlling the draw temperature, preform feed speed, and fiber draw speed such that the thermomechanical scale-down process is performed at high stress where viscous forces dominate and surface energy-driven deformations are kinetically restrained.

A specific example of a surface-patterned amorphous thermoplastic material produced by the FSP approach is illustrated in the inset of Figure 1d, which shows a piece of meter-long patterned PC fiber rolled onto a pencil. This particular fiber is drawn from a preform with milled surface features. The resulting fiber contains sub-5-μm features in the cross section. Figure 1e shows the neck of the preform transitioning from macro to microscale features. Fiber drawing as a high-throughput process is capable of producing km-long flexible, patterned substrates at speeds of tens of meters per minute (Figure 1f). The final fiber size is several hundred microns wide and the feature size on the fiber surface is on the micron scale, both of which can be tuned by altering the DDR (Figure 1g-h). The cross-section image of the patterned fiber is demonstrated in the inset of Figure 1g. See Figure S2 for additional examples of patterned amorphous thermoplastics (*i.e.* PMMA) produced via the laser cutting method.

A particular challenge exists in thermally drawing surface-patterned semi-crystalline polymers. Unlike amorphous polymers which can be drawn at high stress above their glass transition temperature, semi-crystalline polymers undergo a rapid drop in viscosity above their melting temperature, significantly complicating efforts of maintaining non-equilibrium surface features during the draw. To address this challenge, we have developed a 3-step pattern-transfer approach involving molding and fiber drawing (Figure S3). First, a film of

PVDF is sandwiched and thermally consolidated between two rigid PC plates, one of which is patterned with milling and the other untreated. During the consolidation, the PVDF melts and fills the patterns of the PC mold. Second, this sandwiched structure is thermally drawn. During this process, the grating size of the PC mold is reduced and the PVDF liquid follows this size reduction as it is restricted from all sides. While the PVDF is in a low-viscosity state during the draw, the features are maintained due to the highly viscous PC boundaries. The final step involves a simple peeling of the two materials, creating a flexible, surface-patterned PVDF fiber (Figure S3b-c) (along with a complementary surface-patterned PC fiber). This peeling is facilitated by the low interfacial energy at the PVDF/PC interface. It is worth mentioning that this technique enables submicron scale surface patterning of semi-crystalline materials with architectural complexity that is difficult to obtain with other techniques.

A unique feature of FSP is that the uniformity of the patterns both in the axial and transverse directions is well-maintained during the draw, enabling micron and submicron-scale features to extend to kilometer lengths. Figure 2a-b depicts an SEM image of a section of fiber which is used for calculating the size distribution of gratings shown in Figure 2c. The standard deviation of the grating width along 5 meters of the fiber is as small as ~1%. This fiber contains 40 gratings on the surface and the unit cell is ~24 μm (grating width ~8 μm). The fiber could be further redrawn to get iterative size reduction of the features while preserving the uniformity very well (Figure 2d-f). An array of patterned fibers is consolidated on the surface of another preform and then redrawn, generating fibers with submicron features (Figure S4). The standard deviation of the submicron pillar width is calculated to be ~4%. Note that the grating density (number of unit cells per unit fiber width) is increased by redrawing a stacked array of multiple fibers. In particular, a fiber with 1200 unit cells (unit cell = ~1700 nm where the grating width is ~600 nm) is achieved with a single stack-and-redraw step. Gratings with feature size down to 200 nm can be achieved under proper draw conditions (Figure S5-6 for details).

Up to now, we have demonstrated surface patterning of identical, translationally-invariant, rectangular submicron trenches with aspect ratios of the order of 10^{10} (submicron feature along km-long fiber). While that in itself is unmatched by any other fabrication approach, the

FSP process presents other unique opportunities for creating surface patterns of significantly higher complexity. First, a structured gradient surface (SGS) can be designed and fabricated (Figure S7). A SGS refers to a change in either the unit cell periodicity (for example, a chirped grating) or the depth of a surface feature across or along the fiber surface. Such anisotropic surface features are interesting for a number of emerging research topics, including controlling wettability of surfaces, biomedical applications, and others.[28,29] Second, FSP enables the creation of different cross-section feature profiles. For instance, it is possible to produce high aspect ratio (Figure S4f), square, triangular, and hemispherical cross-sectional grating morphologies (Figure S8). Note that the tapered grating features are of importance for a number of applications, in particular in optics, where a tapered average refractive index profile can significantly reduce surface reflections.[30] Third, FSP can be utilized to fabricate hierarchical surface structures comprising patterns at different length scales. The creation of such structures is known to be very challenging using conventional patterning methods such as printing or lithography. With FSP, complex hierarchical structures can be generated by using any of the macropatterning techniques owing to their superior controllability at the macroscale. For example, Figure 2g-h presents hierarchical structures produced by the milling method. The inset shows a single larger unit cell (~tens of microns wide) with smaller unit cells (~ several microns wide) on top of it. Finally, longitudinal features can be added to the fiber patterns using a simple stamping technique. To this end, any patterned molds (including a surface-patterned fiber itself) can be used as a stamp. In this study we use a patterned silicon wafer (Figure S9) to modify 1D fiber gratings post draw. The 1D patterned silicon wafer is pressed onto a 1D patterned fiber as the fiber is heated, thus converting a 1D fiber grating into a 2D pattern as shown in Figure 2i.

Collectively, these FSP tools enable the exploration of a vast phenomenology and application space. Here, we demonstrate two distinct surface phenomena on surface-patterned fibers: diffraction grating and anisotropic wetting. It is known that light diffracts as it passes through a slit with a size comparable to the wavelength of light. This diffraction effect can be observed via optical gratings on the fiber surface. The experimental setup for measuring the diffraction patterns from the fiber is shown in Figure 3a-e. Two fiber samples were measured,

one with micron-class features and one with submicron features. The red laser is transmitted through the patterned fiber, and the diffraction orders can be clearly observed in the far field. The diffraction angle can be calculated by measuring the distance between these orders. A basic calculation using the diffraction formula $n\lambda = D\sin\alpha$ (where n represents diffraction order, λ is the wavelength of light, α is the diffraction angle for different orders, and *D* is the unit cell width) confirms that the *D* values (D_1=23.57 μm and D_2=1.748 μm) match the measurements from the SEM images (D_1=23.67 μm and D_2=1.73 μm) of the micron and submicron patterned fibers, respectively, to within 1%. It is apparent from both the measurement and the calculation that when the width of the unit cell decreases the number of supported orders also decreases and each supported order covers a larger space in the polar domain. This fact, combined with the axial and transverse fiber uniformity, gives rise to the observed vivid coloration when the unit cell becomes comparable to the visible light wavelengths (*i.e.* 400-750 nm). Figure 3f-g shows how the fiber exhibits different colors when viewed from different angles. By weaving surface-patterned fibers we demonstrate angle-dependent chemical-free structural coloration effects over large-area textiles (Figure 3h). An 8-harness satin weave fabric construction was chosen to facilitate maximum fiber surface exposure.

Surface patterned fibers present compelling opportunities for all-structural (non-chemical) control of wetting properties. The multi-channel, micron to submicron scale grating features on the fiber surface induce anisotropic wetting - the wetting behavior is drastically different transverse to the grating pattern compared to along the fiber axis (Figure 3i). As a control, we first investigate the wetting properties of the bare (non-structured) side of the fiber. Here, an isotropic contact angle (CA) value of 90^o is measured, which is in accordance with the CA value measured on PC slabs prior to drawing, confirming that the drawing process itself does not induce anisotropic wetting. However, when placing a water drop on the patterned surface side, the CA in the transverse direction significantly increases (CA=148^o), while in the longitudinal direction the CA is around 91^o, leading to a wetting anisotropy of $\Delta\theta=57^o$. The enhanced hydrophobicity in the transverse direction can be explained by considering the structured surface profile and employing the Cassie-Bexter wetting model. [31] We

hypothesize that this model is applicable to our scenario due to the micron-sized features of the surface structure, the small ratio between grating width to the unit cell, and the fact that the CA increases beyond 90^o for the modified surface. For this type of surface, hydrophobicity is increased due to the trapping of air in the grooves of the grating, thereby increasing the effective interfacial surface energy. It should also be noted that the gratings utilized in this experiment have hemispherical-like edges (which gives even better hydrophobic properties), therefore a modified Cassie-Bexter model should be used for a more accurate estimation of the CA.[31] The contact angle from this model can be estimated by the following formula:

$$(\cos\theta^* = -1 + \emptyset_B(\cos\theta + 1)^2) \qquad (1)$$

where θ is the CA of the bare surface and $\emptyset_B$ is the ratio of the grating surface area to the unit cell surface area. From the cross-sectional SEM image of the fiber used in the measurement (Figure S4f), it is estimated that $\emptyset_B \approx 1/7$ ($\cos\theta = 0\,,\ \theta = 90°$) resulting in the calculation of θ*≈ 149^o, which matches the experimental result to within 1^o.

The anisotropy in the contact angle can be exploited for controlling fluid transport (Figure 3j-k). The potential of anisotropic wetting for facilitating surface-energy-driven fluid flow on the patterned fiber is demonstrated by introducing a flow of fluid onto the surface with the tip of a liquid marker pen. Upon touching the patterned surface, the ink from the marker pen preferably flows along the grating axis while it is restricted along the transverse axis. This enables the simultaneous transport of different fluids on the same fiber surface, as illustrated by flowing different color inks along the fiber without mixing. As a comparison, the axial flow of the ink is not observed when introducing it to the non-patterned bare surface (see Supp. Video 1-2). Importantly, this demonstrates the ability to achieve directional and confined flow on the surface of *individual* fibers without employing any chemical treatments. Moreover, the surface patterned fiber displays water repellency. When the fiber is placed vertically, the anisotropic hydrophobicity and gravity facilitates the flow of water along the grating, thus preventing water droplets from staying on the surface. As a comparison, on the non-patterned side of the fiber, water droplets remain on the surface (See Supp. Video 3-4).

To summarize, a novel and effective method of submicron patterning on flexible polymeric material surfaces is demonstrated. This method is 1) versatile - it can be combined with different surface patterning techniques to treat different types of materials according to their respective properties, and 2) scalable - the thermal drawing process scales down the features of the surface patterns from millimeter to submicron scale, resulting in km-long flexible patterned surfaces. The resulting fiber has many potential applications. Two distinct surface phenomena, vivid structural coloration via the diffraction grating effect and anisotropic wetting, have been demonstrated as enabled by the proposed patterning technique. This surface-patterning fiber technique presents vast opportunities in micro/nano-fluidics, plasmonic metasurfaces, smart surfaces, organic photonics, biosensors, etc. The synergy of the fiber surface patterning coupled with in-fiber functional structures could create more advanced functionalities, paving the way to the development of multi-functional fiber devices and smart textile platforms with increased capabilities.

Supporting Information

Supporting Information is available online from the Wiley Online Library or from the author.

Acknowledgements

The authors are grateful to Marty Ellis at Inman Mills for his efforts on weaving the fibers. This work was supported in part by the MIT MRSEC through the MRSEC Program of the National Science Foundation under award number DMR-1419807 and also was supported in part by the US Army Research Laboratory and the US Army Research Office through the Institute for Soldier Nanotechnologies, under contract number W911NF-13-D-0001. MIT LL contributions were supported by the Assistant Secretary of Defense for Research and Engineering (FA8721-05-C-0002). ((Supporting Information is available online from Wiley InterScience or from the author)).

Received: ((will be filled in by the editorial staff))
Revised: ((will be filled in by the editorial staff))
Published online: ((will be filled in by the editorial staff))

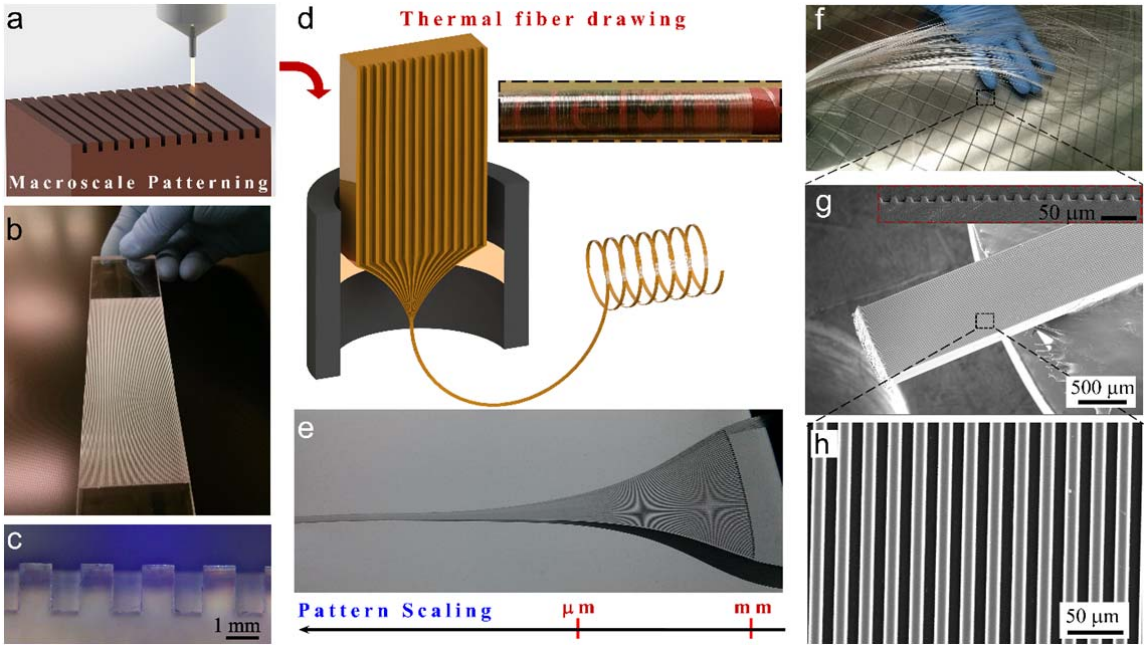

Figure 1. Fiber Surface Patterning. Fiber drawing technique meets macropatterning technologies. (a) Conventional macroscale tools, including milling, laser cutting and molding, are able to process materials at the preform level. (b) Image of a PMMA preform patterned by a laser. (c) Microscope image of the cross section of a PMMA preform patterned by a 1 mm diameter end mill. (d) Thermal fiber drawing reduces the size of the preform as well as the surface patterns. Inset shows several meters of patterned flexible fiber rolled onto a pencil. (e) Preform neck obtained after fiber drawing illustrates dimensional scaling of the process. (f) Continuous strands of patterned fiber are displayed. (g) SEM image of a surface-patterned fiber. Inset represents the cross section of the same fiber. (h) Zoomed-in SEM image of the gratings on the fiber surface.

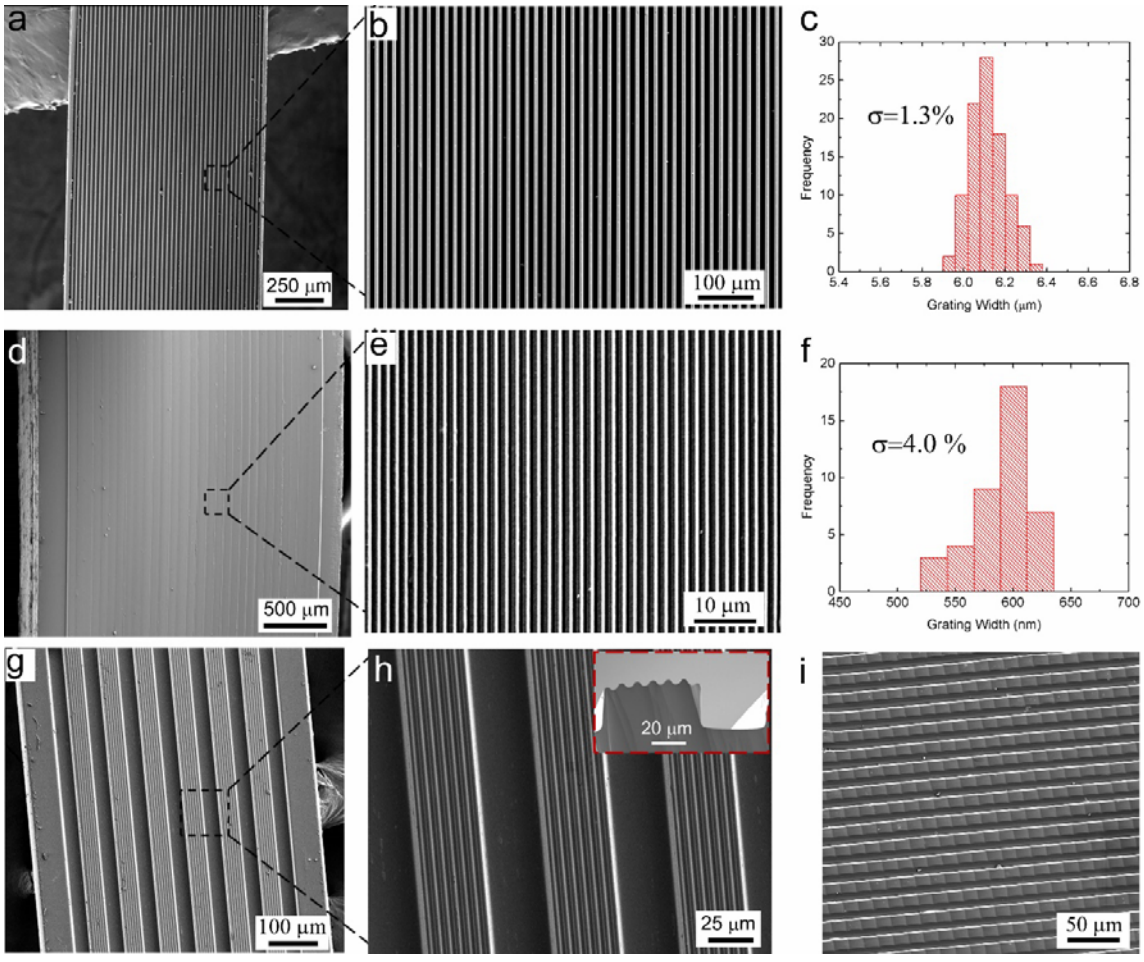

Figure 2. Features of patterned fibers. (a-b) SEM image of a surface-patterned fiber after the first draw. (c) Statistical distribution of the grating size on the fiber in (a-b) is displayed. Exceptional uniformity of patterns is demonstrated on a 5-meter-long patterned fiber. Note that the size distribution includes not only axial but also transverse uniformity of the fiber. (d) The redraw approach facilitates reduction of the patterned dimensions to smaller sizes. The fiber after the redraw process is shown with more than 30 "sub-fibers" stacked on the surface. Those "sub-fibers" are taken from first draw (a-b) and have microscale patterns on their

surface before the redraw. (e) A zoomed-in SEM image shows that the patterns are further reduced to submicron. (f) Statistical distribution of the grating size on the fiber in (d-e) is displayed. Features on the fiber from the first draw are reduced by one order of magnitude and a grating size of ~600 nm is reached. The submicron scale patterns also exhibit good uniformity. (g-h) Hierarchical complexity can be achieved on flexible polymer fibers. Inset of (h) shows zoomed-in image of two different size scales. (i) Post drawing, a stamping process is applied on the fiber surface to generate 2D patterns.

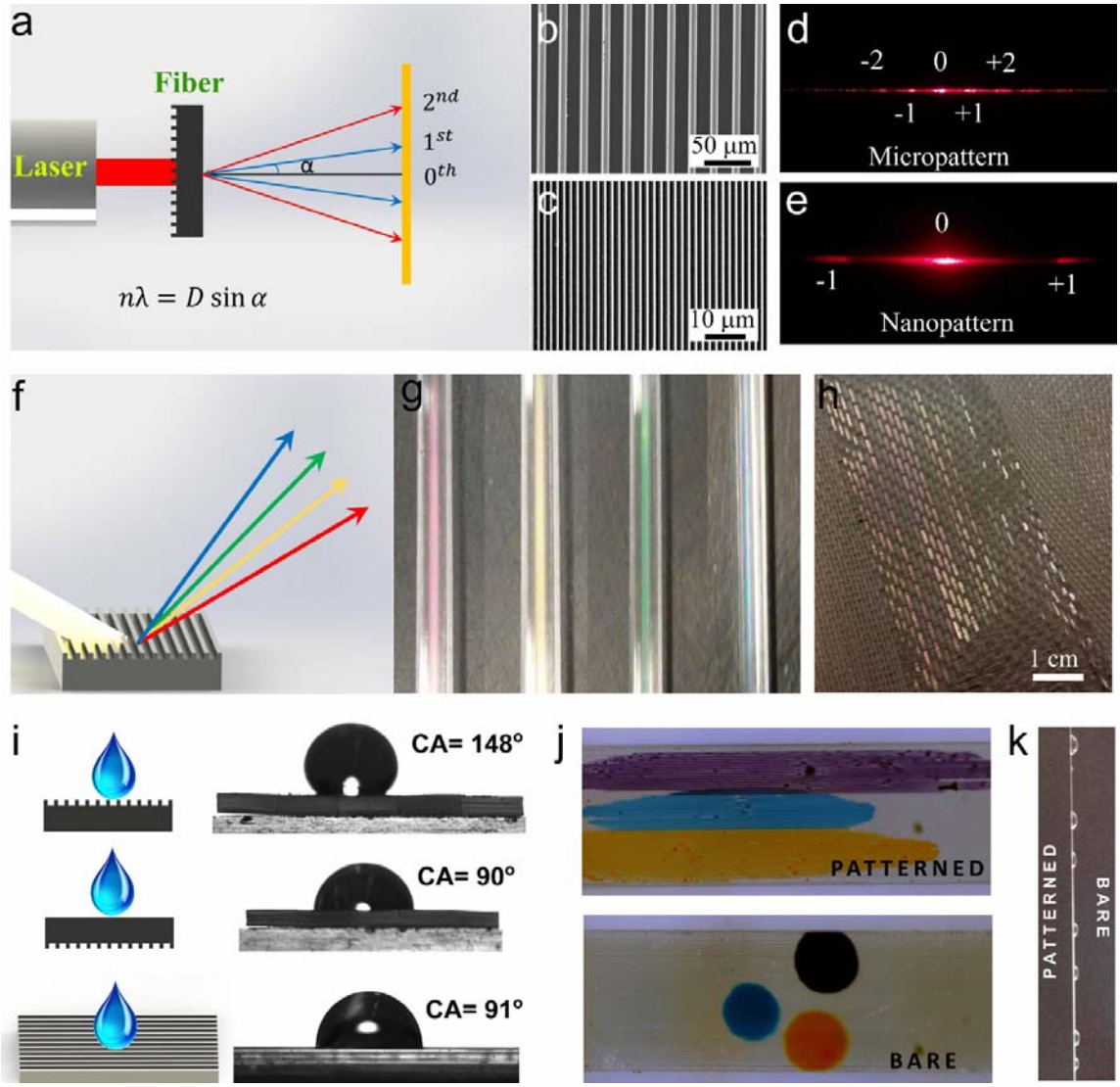

Figure 3. Surface phenomena on patterned fibers and textiles. (a) The patterned fiber surface behaves as an optical diffraction grating when the feature size is comparable with visible light wavelengths. A red laser propagates through the gratings and induces separation of diffraction orders in the spatial domain. (b-e) The diffraction from the micro-patterned fiber has a denser splitting of orders in the polar domain than from the submicron-patterned fiber. (f) Schematic illustration of structural coloration on the patterned fiber surface is shown. (g) The fiber exhibits different colors when viewed from different angles. (h)The surface-patterned fibers are woven into a textile and the textile exhibits large-scale angle-dependent structural coloration. (i) The anisotropic wetting phenomenon is demonstrated on a fiber array (stack of fibers side-by-side) without any chemical treatment. The micro-patterned fiber

surface enhances the hydrophobicity across the patterns (transverse to fiber axis), while the hydrophobicity along the patterned direction (axial) is similar to that of an unstructured surface. (j) Liquid ink is placed onto both surfaces of a single fiber that is ~1 mm wide. The ink spreads along the direction of the micro-gratings right after touching the patterned surface (*See* Supplemental Video 1-2), while on the bare side it does not have directional preference and hence stays in the local region. (k) Water repellency of the patterned fiber surface is demonstrated (Supplemental Video 3-4).

An all-structural fiber surface functionalization technique combining conventional macro-machining and thermal fiber drawing is reported. Ribbon fibers with a variety of submicron surface features extending uniformly over kilometer lengths are produced at rates of tens of meters per minute, enabling a non-chemical, environmentally friendly approach towards functional textiles.

Keyword (grating, fiber, polymer, patterning, textile)

T. Khudiyev, C. Hou, A. M. Stolyarov Y. Fink*

Title (Submicron surface-patterned fibers and textiles)

ToC figure ((55 mm broad, 50 mm high, or 110 mm broad, 20 mm high))

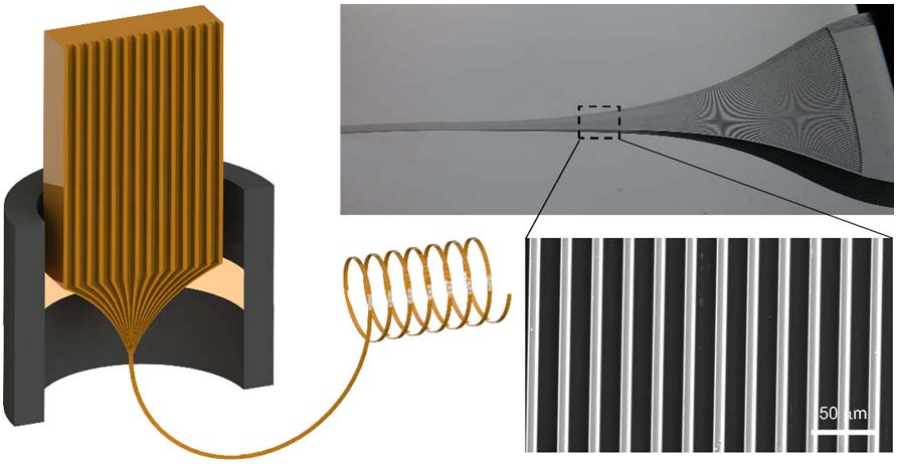

Supporting Information

for *Adv. Mater.*, DOI: 10.1002/adma.((please add manuscript number))

Submicron surface-patterned fibers and textiles

Tural Khudiyev[+], *Chong Hou*[+], *Alexander M. Stolyarov* and *Yoel Fink**

Experimental

Materials and Equipments

The PC, PMMA and PVDF are purchased from McMaster-Carr. The milling of the plastics is done on a TRAK DPM2 type CNC milling machine by Southwestern Industries, Inc. The laser cutting process is done using a CO_2 laser system by Universal Laser Systems, Scottsdale, Arizona, USA. All the SEM images are taken on a JEOL JSM-6010LA. The Contact Angle measurement is taken on a *rame-hart* model 500 from *rame-hart* Instrument co.

Preparation and drawing of a patterned preform with the milling technique

We use a slab of PC which is 1.5" wide and 0.5" thick and use the end mill to cut periodic trenches on the surface. The size of the end mill and the period vary, depending on the designed structure. For example, a 0.5 mm diameter square-shape end mill cutting trenches with a 1 millimeter period would result in a structure with 0.5 mm wide pillars and 0.5 mm wide trenches. The preform is then drawn at a temperature of 260^{o}C with a preform feeding speed of 1mm/min and drawing speed of 2.5m/min. The ratio of the speeds determines the

draw down ratio to be 50. Along with the draw down ratio of 50, the resulting fiber would have a series of 10 micron wide pillars spaced by 10 microns from each other.

Preparation and drawing of a patterned preform with the lasing technique

PMMA is a polymer that is cut with a laser. We utilize a 1.5" wide and 0.25" thick PMMA plastic slab. One advantage of laser cutting is its fast processing speed; however, the resulting pillars are not as rectangular as the ones cut by end mills. The PMMA normally gets ablated more at the surface, and the ablation is reduced at deeper penetration depths below the surface. This results in trapezoidal patterns in cross section. The PMMA is drawn at 240^{o}C with similar preform feeding and drawing speeds as PMMA. After drawing, the trapezoidal shape is maintained and the pillar size shrink with the same scale as the draw down ratio.

Preparation and drawing of a patterned preform with the molding technique

A piezoelectric material, polyvinyl difluoride (PVDF), is utilized to demonstrate this molding technique. A PC plate is used for the mold, and the desired pattern is milled into this PC plate. The PVDF is then embedded between this PC slab and another non-machined PC slab. The whole assembly is heated to 180^{o}C to consolidate the structure. This temperature is only slightly above the PC glass transition temperature so that the PC maintains its shape nearly perfectly. However, this temperature is much higher than PVDF's melting point so the PVDF melts and fills the space between the pillars on the PC surface. The consolidated preform is then thermally drawn and the pillar array structure inside the preform is scaled down into a micron-scale structure within a PC-clad fiber. Since the PC and PVDF do not stick to each other very well, the PC-clad fiber can be easily peeled into two parts, one containing the PC with surface patterns and the other containing the PVDF with surface patterns. In this way the PVDF is also successfully patterned on the surface with micron-scale features.

Characterization of the optical fiber gratings

For the first diffraction order of the micron and submicron patterned fiber, we utilize the formula $\alpha = \tanh^{-1}\frac{s}{L}$ (where s represents distance from 0th order to 1st order and L is the

distance between fiber and light detection plane) to find the angle of diffraction. In our case s=6 cm and L=216.3 cm for micron-patterned fiber, while s=7.5 cm and L=18.5 cm for the submicron-patterned fiber. We calculate α_m=1.586^o and α_n=22^o for the micron and submicron scale patterned fibers, respectively. By using the diffraction formula for the first diffraction order (n=1), λ=655 nm and the measured diffraction angles, D spacing values of 23.57 μm and 1.748 μm can be found for the micron and submicron scale gratings, respectively. From SEM images we extract D values of 23.67 μm and 1.73 μm, which are very close (within 1%) to the values obtained from the diffraction experiments.

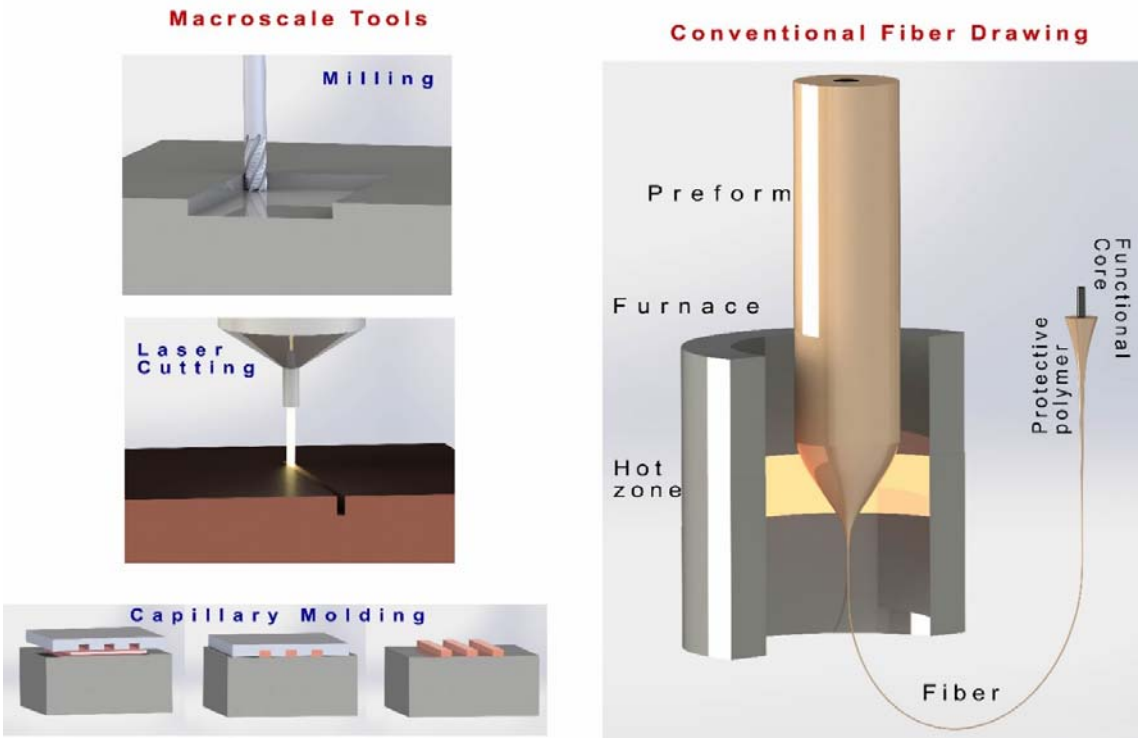

Figure S1. A conventional fiber drawing approach and macroscale machining of materials is shown. Laser cutter, CNC milling and molding are common methods to define macroscale features on the surface of materials. The conventional fiber drawing approach utilizes a cylindrical fiber geometry where the outer polymer region supplies flexibility and protects the functional core materials from fracturing (after or before drawing) or leaking/deforming (during drawing).

Milling, laser cutting and molding are very important tools and have been successfully utilized for machining materials at the macro scale (Figure S1). There are several critical

factors relevant to obtaining well-defined and uniformly patterned fibers. A rectangular preform (instead of the conventional cylindrical) is more convenient for patterning due to its planar surfaces. Therefore, to achieve good patterning results, we utilize rectangular preforms with superior surface roughness. The tough nature of the macroscopic plastic preform prevents any type of distortions from occurring during the registration of features. This circumvents the stability issues typically encountered when having to directly pattern thin plastic films.

Current CNC milling technology allows programmable and customized patterning of surfaces with feature sizes as small as several tens of microns. However, at this very small size scale, the process is very slow and the end mill becomes very fragile. Therefore, there is a tradeoff between the efficiency (*i.e.* time, durability) and the scale. Hence, sub-mm sizes are considered as an optimal working region. Furthermore, although the laser cutting method can efficiently pattern PMMA, rubber, polypropylene, polyoxy-methylene, polyester, fluoropolymers, nylon-type polymers, it is inappropriate for cutting other polymers (*e.g.* PC, PI, PVC) where milling can be used to machine the preform. The laser cutting method is also programmable as the milling method, except that the depth of the cut is defined by the laser power.

The second step in the proposed patterning technique is a thermal fiber drawing approach that maintains the surface morphology of the patterned preform while allowing it to scale down in feature size. The thermal fiber drawing technique is a mature approach. It has achieved many milestones, including the fabrication of telecommunication fibers, the emergence of multimaterial fibers, [32] and more recently the production of arrays of nanowires [33] and nanospheres [34]. However, in all of these designs, researchers have mastered how to functionalize the interior of the fiber. To date, however, the exterior fiber surface has not been well studied [35,36,37] even though it is as important as the interior. In the conventional fiber drawing technique (Figure S1), the outer polymer generally provides

flexibility and protects the functional core from breaking or deforming during the draw. Heat builds up inside of the core materials through conduction from the outer polymer and makes it soft. Even though the outer preform surface is closest to the furnace heating elements, the surface heating is a transient process, and there is additional natural convection (or optional cooling in our case via directed nitrogen flow over the surface) on the outer region that prevents heat buildup on the surface. We utilize this advantage and manage heat flow on the surface of the fiber during the draw, thus enabling complex surface features to be maintained as the preform necks down into the fiber.

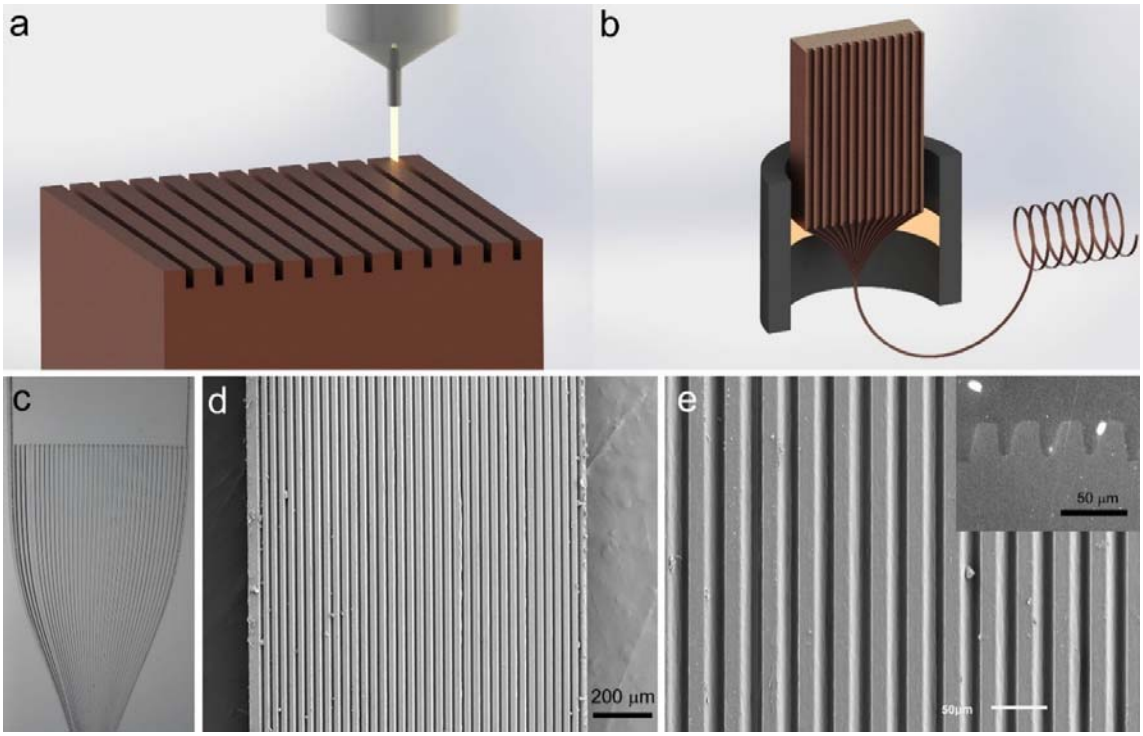

Figure S2. The laser cutting method with fiber drawing is shown. (a,b) The processing of a plastic PMMA preform with the CO_2 laser cutting method and drawing of the patterned preform is depicted. The drawing process enables the fabrication of a wide range of patterned sizes by controlling the draw down ratio. (c) The preform neck after drawing of the PMMA is shown. (d,e) SEM images of patterned PMMA fiber are depicted. The inset shows the cross-section of this fiber.

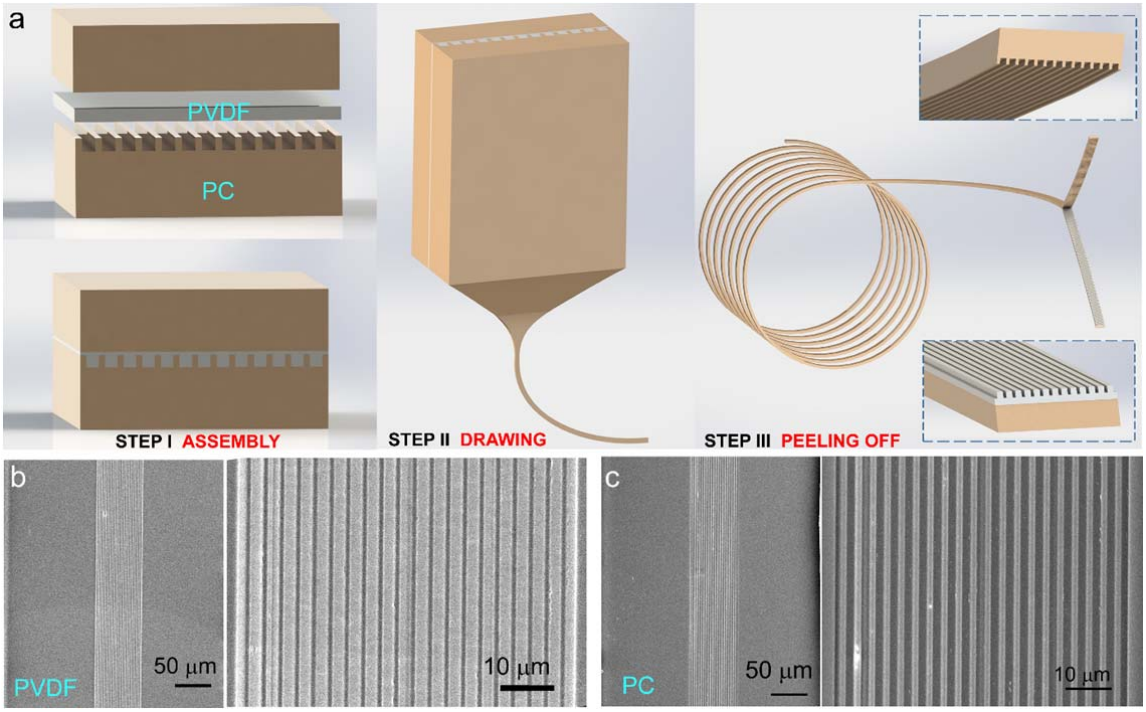

Figure S3. The molding method with fiber drawing for surface pattering of semi-crystalline materials is depicted. (a) PVDF film is sandwiched between a patterned PC slab (which functions as the mold) and a bare PC slab (which restricts the PVDF material from the other side). The PVDF melting temperature is lower than the PC glass transition temperature;therefore the PVDF melts and fills the holes of the mold at the macroscale, where flow of viscous material is relatively easier compared to the micro/nanoscale. The sandwiched preform is then drawn in a fiber draw tower where both the features of the mold and the molded material are simultaneously reduced. After drawing, the fiber is easily peeled thanks to non-adhesive property of the PVDF polymer. SEM images of the patterned (b) PVDF (molded) and (c) PC (mold) fiber show micron-scale surface features.

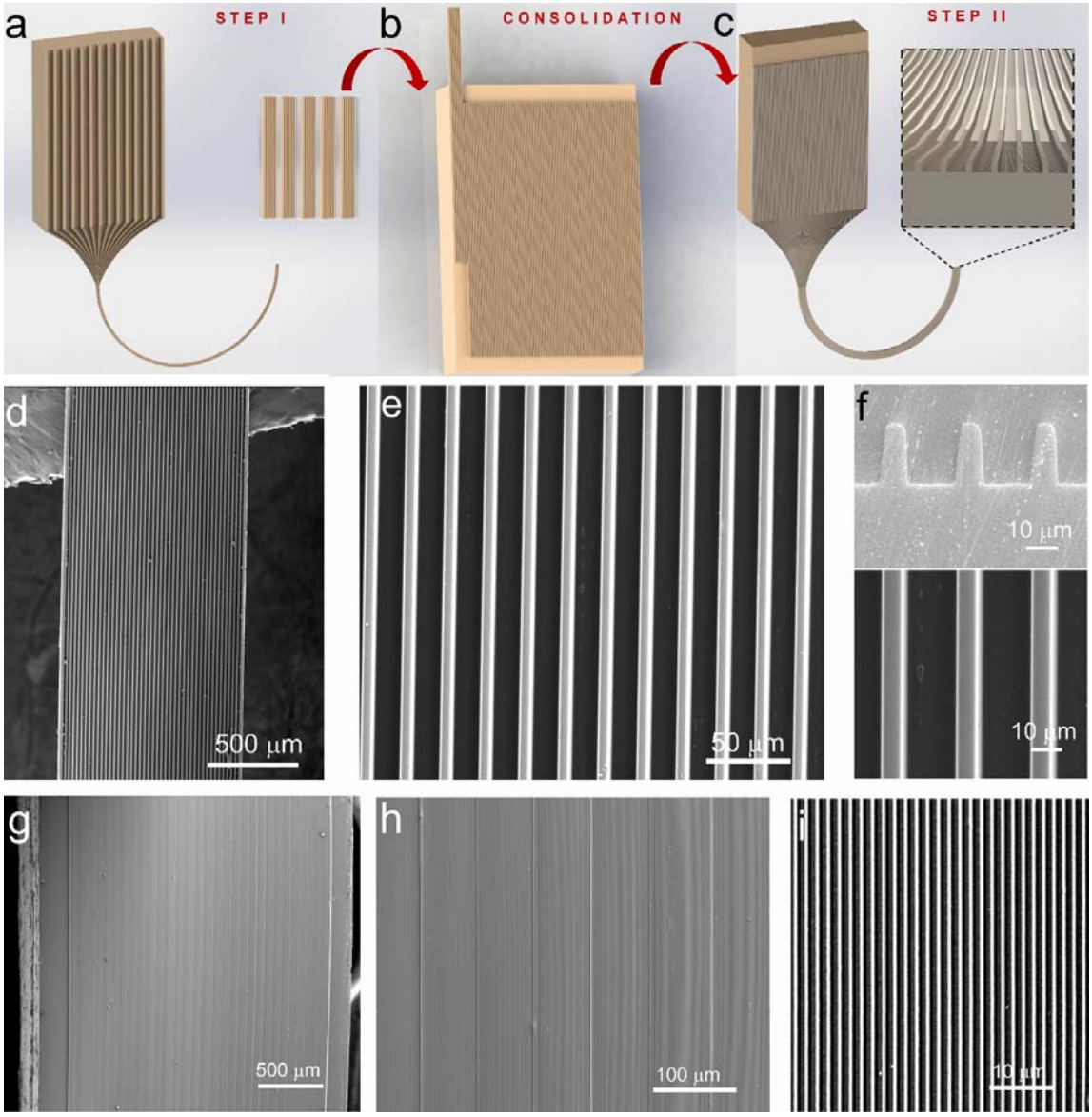

Figure S4. The redraw technique for nanoscale patterning is shown. (a) The first drawing step utilizes the macroscale preform, patterned with milling. The preform size is reduced by a draw down ratio of about 40. (b) The drawn fibers are cut and then assembled and consolidated on the surface of a second macroscale bare (unpatterned) preform. (c) The second drawing step is performed in a similar way as the first. Nanoscale features are achieved at the end of two iterative drawing steps. (d-f) SEM images of fibers after the first drawing step. (g-i) SEM images of fibers after the second drawing step. More than 1000 nanogratings are obtained after the second drawing step.

As a result of the iterative size reduction approach, the production of sub-5 nm features has been demonstrated in previous studies [38]. In the conventional redrawing technique, the fiber produced from the first drawing step is inserted inside a hollow preform to redraw it. Here we modify this technique and consolidate arrays of patterned fibers on the surface of a second preform (instead of inside) and similarly repeat the fiber drawing process (Figure S4a-c). Results of the first step of fabrication with 40 gratings with a size of ~8 μm is shown in Figure S4d-f. More than 30 fibers are then used in step II and submicron scale features of ~600 nm are obtained after the re-draw (Figure S4g-i). It is possible to increase the draw down ratio to decrease the grating size even further. We utilize nitrogen gas and locally cool the patterned region of the fiber during the draw to produce better surface morphologies (Figure S5). Cooling with gas induces forced convection on the fiber surface and hence balances the viscosity of the grating region with that of the bulk region beneath the surface. Depending on the requirements for a particular application, the features can potentially be reduced much further by optimizing the drawing conditions with advanced surface cooling strategies (*e.g.* optimizing nitrogen flow rates and the spatial distribution of the flow).

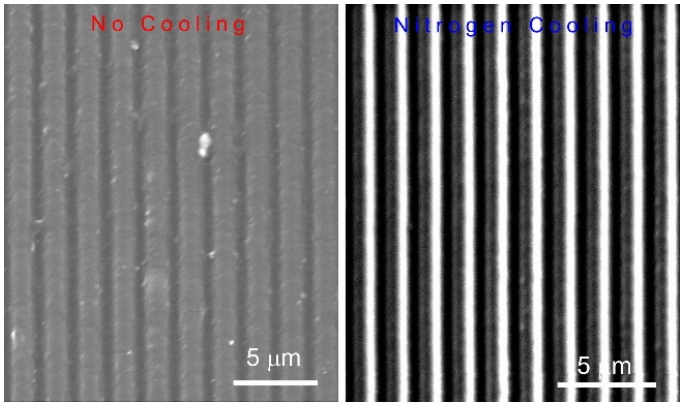

Figure S5. The effect of nitrogen cooling on the grating profile is demonstrated. When the fiber surface features are reduced to the submicron class, the surface heat induces

morphological changes on the gratings. In order to minimize this side effect, we utilize surface cooling (i.e. nitrogen gas flow) to balance surface viscosity with the base substrate.

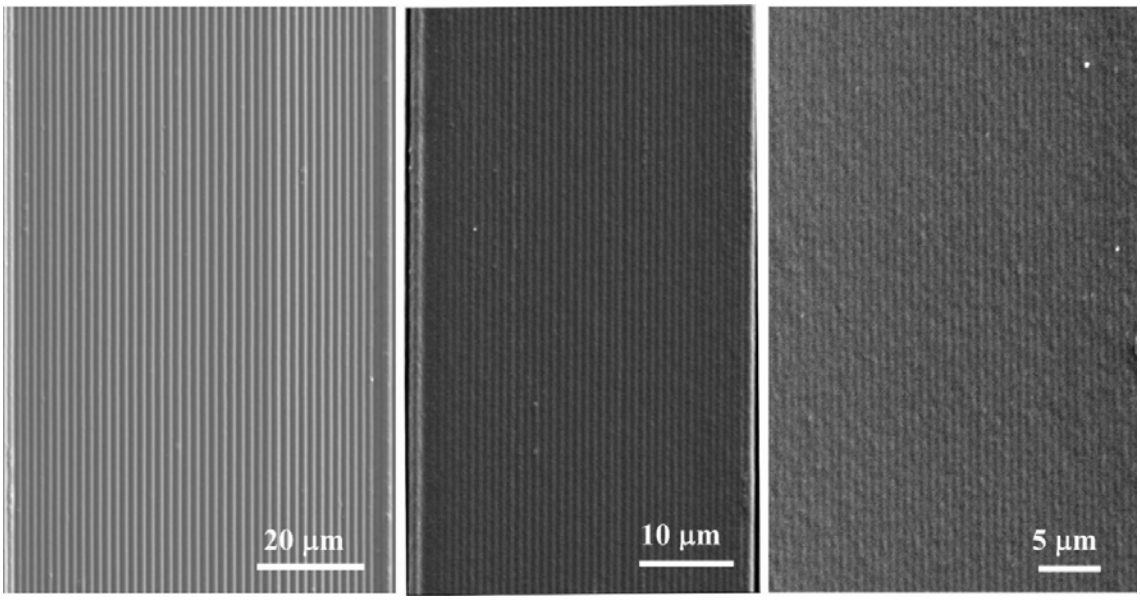

Figure S6. The redraw approach is used for reducing the surface patterns to the nanoscale. Smaller features are obtained by increasing the preform-to-fiber draw down ratio. Grating sizes of ~600 nm, ~250 nm and ~200 nm are demonstrated (from left to right).

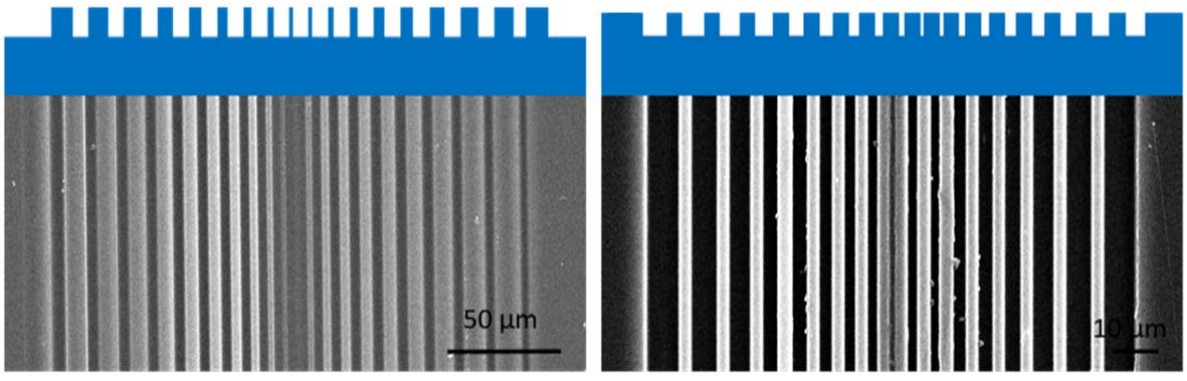

Figure S7. A chirped grating structure is demonstrated, serving as an example of a structural gradient surface on a fiber. Using macro-machining methods, both the height and the periodicity of trenches can be arbitrarily varied. The fiber drawing process then elongates the macroscale preform into a fiber with the desired size while preserving the original gradient

scheme. Even though fabrication of gradient surfaces is considered to be challenging, our method allows facile production of these structures.

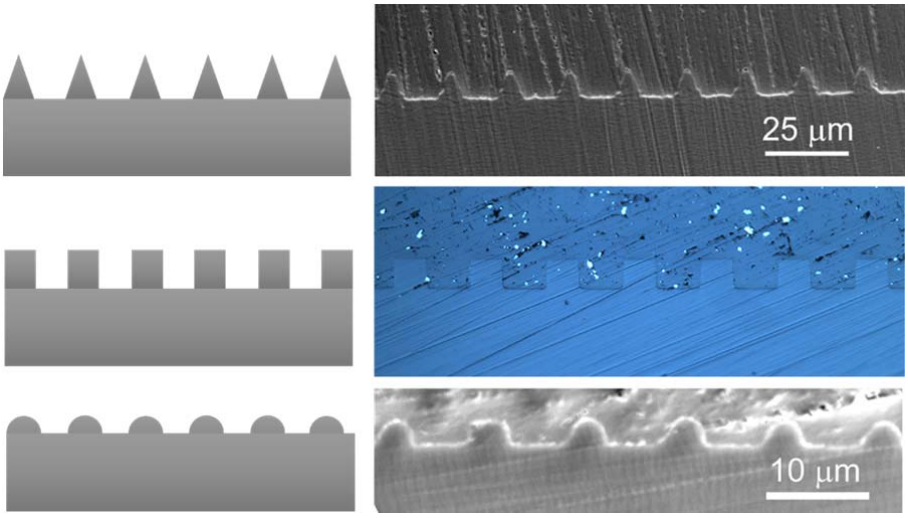

Figure S8. Different grating cross-sections are achieved. Different grating profiles, including triangular, square and hemispherical shapes are demonstrated on the fiber surface. Note that the hemispherical feature is obtained by intentionally drawing a preform with square cross-sectional features at low stress (low viscosity). In this regime, surface energy minimization drives the natural tapering of the square features into hemispherical ones.

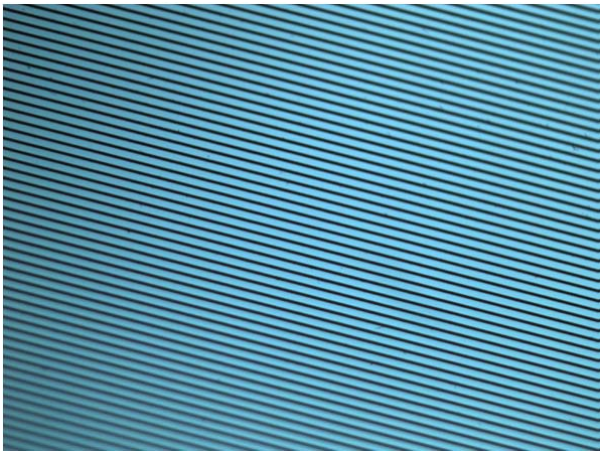

Figure S9. The silicon mold used for making 2D patterns is shown. One dimensional patterns created on the surface of the fiber can be converted into 2D features by applying a 1D mold in

the transverse direction. A silicon wafer that consists of a 1D grating array is utilized for this purpose.

[1] Industrievereinigung Chemiefaser. Worldwide production volume of chemical and textile fibers from 1975 to 2015 (in 1,000 metric tons). https://www.statista.com/statistics/263154/worldwide-production-volume-of-textile-fibers-since-1975/ (accessed October 26, 2016).

[2] W. S. Perkins, *Textile coloration and finishing.* Carolina Academic Press, Durham, North Carolina, United States. **1996**.

[3] W. D. Schindler, P. J. Hauser, *Chemical finishing of textiles.* Elsevier. **2004**.

[4] B. Simoncic, B. Tomsic, *Text. Res. J.* **2010**, *80,* 16,

[5] N. Abidi, L. Cabrales, E. Hequet, *ACS Appl. Mater. Interfaces* **2009,** *1*, 10,

[6] K. L. Hatch, H. I. Maibach, *J. Am. Acad. Dermatol.* **1995**, *32,* 4,

[7] International Agency for Research on Cancer, Some flame retardants and textile chemicals, and exposures in the textile manufacturing industry. *IARC monographs on the evaluation of carcinogenic risks to humans*, **1990,** 48,

[8] R. Kant, *Nat. Sci.* **2012**, *4*, 1,

[9] H. M. Pinheiro, E. Touraud, O. Thomas, *Dyes Pigm.* **2004**, *61*, 2,

[10] M. Kobya, E. Demirbas, O. T. Can, M. Bayramoglu, *J. Hazard. Mater.* **2006**, *132*, 2,

[11] K. Lacasse, W. Baumann, Textile Chemicals: Environmental data and facts. Springer Science & Business Media. **2004,**

[12] A. K. Verma, R. R. Dash, P. Bhunia, *J. Environ. Manage.* **2012**, *93*, 1,

[13] Z. Wang, K. Huang, M. Xue, Z. Liu, Textile dyeing wastewater treatment. *INTECH* Open Access Publisher 2011, pp. 91-116

[14] Swedish Chemicals Agency. 2014. Chemicals in textiles. Risks to human health and the environment. Report 6/14.

[15] S. Khan, A. Malik, In Environmental Deterioration and Human Health: Natural and anthropogenic determinants; A. Malik, E. Grohmann, R. Akhtar, Eds.; Springer Netherlands: Dordrecht, 2014; pp. 55–71.

[16] F. Uddin, *Am. J. Energy Res.* **2014**, *2*, 53–59.

[17] D.Y. Kim, S.K. Tripathy, L. Li, J. Kumar, *APL* **1995,** *66,* 10,

[18] J. Bico, U. Thiele, D. Quéré, *Colloids Surf., A.* **2002**, *206*, 1,

[19] N. Meinzer, L. B. William, I. R. Hooper, *Nature Photon.* **2014**, *8*, 12,

[20] R. Gillibert, M. Sarkar, J.F. Bryche, R. Yasukuni, J. Moreau, M. Besbes, G. Barbillon, B. Bartenlian, M. Canva, M. L. de La Chapelle, *Nanotechnology* **2016,** *27*, 11,

[21] S. J. Park, M. L. Seol, S. B. Jeon, D. Kim, D. Lee, Y. K. Choi, *Sci. Rep.* **2015**, *5*,

[22] Y. Ito, *Biomaterials* **1999**, *20*, 23,

[23] M. Geissler, Y. Xia, *Adv. Mater.* **2004**, *16*, 15,

[24] T. Betancourt, L. Brannon-Peppas, *Int. J. Nanomedicine* **2006**, *1*, 4,

[25] E. Menard, M. A. Meitl, Y. Sun, J. U. Park, D. J. L. Shir, Y. S. Nam, S. Jeon, J. A. Rogers, *Chem. Rev.* **2007**, *107*, 4,

[26] Z. Nie, E. Kumacheva, *Nat. Mater.* **2008,** *7*, 4,

[27] J. F. Ready, D. F. Farson, eds., *LIA handbook of laser materials processing* Orlando, FL: Laser Institute of America **2001**.

[28] S. Inagi, *Polymer Journal*, **2016,** *48*, 1,

[29] J. Genzer, John Wiley & Sons. ed., **2012**.

[30] B. Daglar, T. Khudiyev, G.B. Demirel, F. Buyukserin, Bayindir, M., *J. Mater. Chem. C* **2013**, *1,* 47,

[31] J. Bico, C. Marzolin, D. Quéré, *EPL* **1999**, *47*, 2,

[32] A. F. Abouraddy, M. Bayindir, G. Benoit, S. D. Hart, K. Kuriki, N. Orf, O. Shapira, F. Sorin, B. Temelkuran, Y. Fink, *Nat. Mater.* **2007**, *6*, 5,

[33] M. Yaman, T. Khudiyev, E. Ozgur, M. Kanik, O. Aktas, E. O. Ozgur, H. Deniz, E. Korkut, M. Bayindir, *Nat. Mater.* **2011**, *10*, 7,

[34] J. J. Kaufman, G. Tao, S. Shabahang, E. H. Banaei, D. S. Deng, X. Liang, S. G. Johnson, Y. Fink, A. F. Abouraddy, *Nature* **2012**, *487*, 7408.

[35] A. Yildirim, M. Yunusa, F. E. Ozturk, M. Kanik, M. Bayindir, *Adv. Funct. Mater.* **2014,** *24*, 29,

[36] T. L. Lowder, B. R. Tebbs, R. H. Selfridge, S. M. Schultz, K. H. Smith, T. D. Monte, *Appl Opt.* **2007**, *46*, 13.

[37] Â. L. Andrade, R. M. D. M. Turchetti-Maia, M. T. P. Lopes, C. E. Salas, R. Z. Domingues, *Materials Research* **2004**, *7*, 4,

[38] J. J. Kaufman, G. Tao, S. Shabahang, D. S. Deng, Y. Fink, A. F. Abouraddy, *Nano Lett.* **2011**, *11*, 11.